Nuclear Counting

Adam Colin Eagles, Andy Chmilenko
Instructor: Jeff Gardiner
Section 1
(Dated: 1:30 pm Monday October 21, 2013)

I. ABSTRACT

The Geiger-Mueller tube is a popular and simple radiation counter capable of detecting multiple types of ionizing radiations and their relative strengths. The properties of the G-M tube as well as the properties of radiation like its random nature, and the ability for materials to block radiation will be investigated in this experiment. We were able to compare two different tubes and observe the counting plateau as we increased the voltage and observed the subsequent count rate. Selecting a tube to use for the rest of the experiment, we measured the dead time to be about 28 μs. We were able to observe the random nature of radioactive decay and apply it to Possion/Gaussian statistical laws. We were also able to determine the range of the β-particles from a source and their associated energy to be 200 $\pm 20 mg/cm^2$ and 0.6 $\pm 0.5 MeV$ respectively. The measured energy only differed from the accepted value of 0.709MeV, by only a 15% difference.

II. INTRODUCTION

The Geiger-Mueller tube is one of the oldest radiation detector types in existence, it was introduced by Geiger and Mueller in 1928 hence the name. It was one of the most popular tools for detecting radiation due to its simplicity, the low cost of manufacturing, and its ease of operation.

We will be investigating the properties of the G-M tube using β-particle emitting sources, such as the counting plateau, the point at which the count rate is very loosely proportional to the change in voltage to the tube by measuring the count rate for a set sample at different voltages of operation. We will also be measuring the dead time of the tube using the two source method, measuring the count rate of each source individually then together for a set of voltages then averaging the results. The two source method allows a series of equations related to the dead time to be built and used to solve for T, the dead time. Knowing the dead time is important because this is a period during which the tube cannot register new counts. Knowing this allows us to better describe the radioactivity of the sources being measured and comparing strong sources with weak sources.

Also using the G-M tube we will investigate the properties of radioactive sources, like the random nature of radiation by measuring the number of counts in a set time for many trials and applying our measurements to statistical laws to radioactive emission rates of sources. We will also look at the ability of Aluminium to absorb β-particles from a source and use this to determine the range of β-particles in Aluminium, as well as the maximum energy of emitted particles from our sources by measuring the count rate of a source behind an aluminium blocker for of different widths, and plotting the count rate values versus the thickness of the absorber.

Knowing these properties can lead to many important advances in manufacturing for medical, commercial, and scientific equipment as radioactivity and nuclear power is becoming more prolific in our society today and probably even more so in our future.

III. THEORETICAL BACKGROUND

The Geiger-Mueller Counter

The Geiger-Mueller tube consists of a sealed tube with a window on the bottom face that allows particles into the tube, with a wire running down the middle inside. The tube is filled with usually a noble gas (due to its filled outer electron shell) and to a lesser degree, a quenching gas whose purpose will be explained shortly. An external circuit is usually part of the tube operation as an external quenching mechanism as well.

During operation, the tube and the wire are charged, to create an electric field inside the tube, with the tube being the cathode and the wire the anode. With the electric field inside the tube at a radius r given by:

$$E(r) = \frac{V}{rln(\frac{b}{a})} \tag{1}$$

where $a \equiv$ anode wire radius, $b \equiv$ cathode inner radius, and $V \equiv$voltage between the anode and cathode.

The process which the G-M tube detects ionizing radiation, is the process where the noble gases inside the tube are ionized producing an electron and a positive gas ion, which travel to the anode and cathode respectively. This electrical pulse in the unit can be detected as an ionization event, or a count from a radioactive source. For the pulses to be have a significant enough voltage to measure the G-M tube relies on the phenomenon of gas multiplication to amplify the effect of a single ionization event.

When an electron and ion pair are created, and in the large potential E-field of the G-M tube start to travel to their respective electrodes, the electron can hit another neutral noble atom producing another electron and ion pair, resulting in two electrons which may repeat this process toward the anode. This process is called a Townsend avalanche. However, the gas molecules will quickly return to their ground state, emitting a photon which can ionize another atom within the tube or liberate an electron from the tube wall, each of which result in another avalanche of electrons, which in turn, can create other avalanches within the G-M tube. This is the process of gas multiplication which can turn a single ionization event from a β-particle into many events, creating an electrical pulse strong enough to easily detect, this process is roughly illustrated in Fig.1.

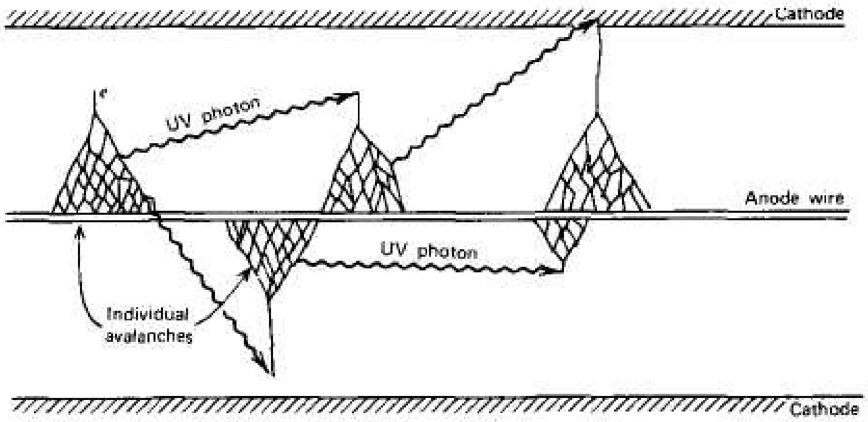

FIG. 1: Illustration of individual Townsend avalanches and the mechanism of gas multiplication in a crossection of a G-M tube, with the other cathode tube walls illustrated on the top and bottom, and the anode wire down the middle [1]

Since the time required to spread these avalanches is short and they only begin when the free electron and drifted to within a few mean free paths of the anode wire, the time it takes for the avalanches to grow in both directions along the wire only takes a small fraction of a microsecond. Since positive ions travel much slower than the electrons do, due to their mass, a high concentration of positive ions collect and sufficiently nullify the E field in the vicinity of the wire, and free electrons will no longer have a high enough ionization potential to create more avalanches until the cloud of positive ions travel outward to the cathode and equilibrium is restored to the tube, to a sufficient degree to create avalanches again during an ionization event. This period where the tube cannot create more avalanches is called the Dead Time as shown in Fig.2.

---

[1] Image from Radiation Detection and Measurement, by Glenn F.Knoll, © John Wiley, N.J

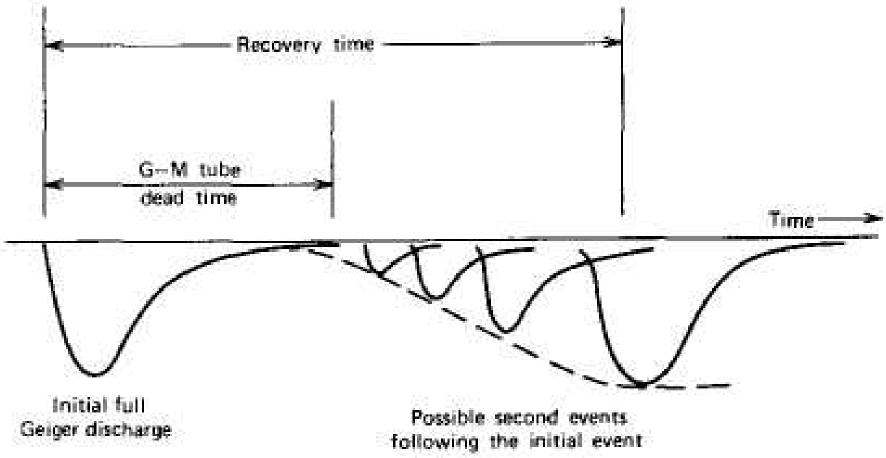

FIG. 2: Graph representing the dead time of a G-M tube, and it's subsequent recovery thereafter, and the amplitude of possible subsequent pulses during the recovery time [2]

The gasses inside the G-M tube is largely filled with a noble gas because of their neutral charge in inert nature, in our case the noble gas filling the G-M tubes is Neon. A secondary gas is also put into the tube for the purpose of internal quenching. After a discharge, as the positive ions are drifting toward the inner tube wall and becoming neutralized by combining with an electron from the cathode surface, if the difference of that atoms ionization energy and work function of the cathode is greater than the work function of the cathode surface, there is a small chance that an extra electron can be liberated which can cause a Townsend avalanche leading to the G-M discharging again. To fix this there is the process of quenching, externally through a circuit which happens after discharging, the circuit reduces the high voltage applied to the tube for a small fixed time after the pulse using a capacitor circuit, this stops the process of gas multiplication so secondary avalanches cannot be formed. There is also the method if internal quenching, which uses a quench gas (as mentioned previously) in lower concentrations with the primary noble fill gas (about 5-10%) which has a lower ionization potential, its purpose is to stop multiple pulsing through charge transfer collisions. As the positive ions of the primary gas, while drifting toward the cathode, collide with the quench gas molecules, because of the lower ionization energy the positive charge is transferred to the quench gas molecule and the primary gas atom becomes neutral. If the concentration of the quench gas is sufficient, only quench gas molecules will be neutralized at the tube surface and because of the lower ionization energy the probability of dissociation is larger than the liberation of a free electron. In our case, a Halogen gas is used as the quench gas.

When looking at the charge on the tube versus the count rate, it is obvious that when the charge is below a certain threshold that there will be no recorded count rate, when the count are first recorded this is called the starting voltage, and the count rate increases rapidly as the voltage is increased up to a point where the rate plateaus. Increases the voltage doesn't change the count rate by any significant amount. There will be a point though, a critical voltage value above this where the G-M tube will continuously discharge, which may damage the tube. This plateau generally has a slope of 2-10% per 100V.

Determination of the Dead Time

If we assume a β-particle emitter gives N counts per second, with zero dead time, and n counts per second with a counter with a dead time of T seconds. So the counter cannot detect nT counts within this period, so the dead time is equivalent to:

$$N_i - n_i = N_i n_i T \tag{2}$$

Using two sources, we can build up a system of equations for the count rates with each source individually and one with the two sources measured together. Solving for T we can find T to be:

[2] Image from Radiation Detection and Measurement, by Glenn F.Knoll, © John Wiley, N.J

$$T \approx \frac{n_1 + n_2 - n_3}{2n_1 n_2} \tag{3}$$

with a factor of $O(nT)^2$ to be omitted, and it is assumed at the counts are generally equally space in time.

Random Nature of Radioactive Decay

Due to the random nature of radioactive decay, only the mean count rate can accurately describe the count rate over large period of time. The count rate over time follows a Poisson distribution, which can be approximated with a Gaussian distribution. σ, is the square root of the averages of the squares of the deviations from the mean count m, which is equal to the square root of the mean count. The probability of the relative error between t and $t + dt$:

$$P_o(t)dt = \frac{e^{-\frac{t^2}{2}}dt}{\sqrt{2\pi}} \tag{4}$$

where,

$$t = \frac{n - m}{\sigma} \tag{5}$$

and n $\equiv$ measured count, and m $\equiv$ mean count, and sigma $\equiv$ square root of the mean count.

Absorption and Range of β-Particles in Aluminium

The ability of a material to absorb or block radiation to a first approximation is independent of atomic number, the ability proportional to the thickness of the material in terms of density. For example, 0.5 mm of lead absorbs beta particles about the same as 2 mm of aluminium, since they both have a thickness of 570 mg/cm^3. Using aluminium is easier to use at small thicknesses because lead has a very low ductility, while aluminium is, meaning the absorbers can me more accurately made.

If the count rate versus the absorber thickness is graphed, with the count rate on a logarithmic scale, a graph such as Fig.3 will be seen. The tail of the graph is due to γ radiation, also known as bremsstrahlung radiation produced from the β-particles being absorbed in the aluminium. The graph can be extrapolated downward (also shown in Fig.3) to a point which represents the the thickness where the maximum energy of the particles emitted from the source are completely blocked.

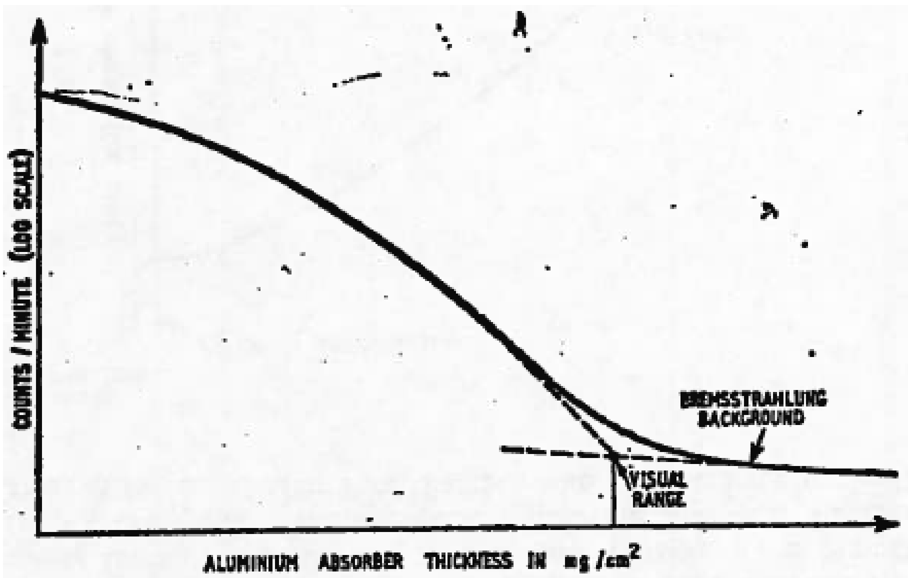

FIG. 3: Log count rate versus absorber thickness [3]

IV. EXPERIMENTAL DESIGN AND PROCEDURE

Characteristics of Geiger Tubes

A single source of Chlorine-36 was placed under the Geiger tube and enclose within a lead stack to minimize background the effect of background radiation. The Geiger tube was attached to a power supply as well as a voltage measuring device and a counting device. Allowing the operating voltage to be determined and the count and voltage to be read by the system. A computer was attached to the voltage measuring and counting devices, allowing much of the measurements to be automated. To determine the characteristics of the two supplied Geiger tubes, LND 712 and LND 72314 models, we loaded a program that would measure the total count over a specified time interval. We set the time interval for 60 seconds and measured the total at a number of different operating voltages. These voltages ranged from 300-650V for the LND 712 model and from 300-700V for the LND 72314 model, in increments of 25V. From this data we were able to plot a graph relating the radiation count to the operating voltage and thus decide on which tube and voltage would be suitable for the subsequent tests. The subsequent tests were completed using the LND 72314 model at an operating voltage of 575V.

Measuring the Dead Time

To measure the dead time we used a dual source of β Chlorine-36 in the same arrangement as the single source for the previous test. Using the LND 72314 Geiger tube at an operating voltage of 575V we measured the amount of radiation detected in 60 second intervals. We took four separate readings for the background, first source, second source and both sources. The test was repeated 5 times to increase reliability.

Statistics of Radioactive Decay

For statistical analysis of the regularity of the radioactive decay we performed a number of measurements of the number of counts in a small time interval. The time interval used was calculated according to the formula

$$T_i = T_0 \cdot \frac{20}{N_0} \tag{6}$$

where T_0 and N_0 are the time interval and count from the first experiment. By using this time interval the expected value for the radiation emitted is 20 counts. Thus allowing us to test the variance from this figure. Substituting values into eq. 6

$$T_i = \frac{60 \times 20}{4629} = 0.259s$$

In each test we measured the count over the time interval N times, where N = 10,100,300,500.

Range of Beta Particles in Aluminium

To measure the range of the β particles through aluminium we performed measurements of the amount of radiation detected in 60 seconds for various thicknesses of aluminium shielding. The shields were placed above the source in the stack, ensuring that when changing the shield the Geiger tube wasn't exposed to the source alone. This is to eliminate the possibility of hysteresis errors.

---

[3] Image from Counting Systems handout, Brown

V. ANALYSIS

Characteristics of Geiger Tubes

The relations between applied voltage and radiation count for the LND 712 and LND 72314 Geiger tubes are plotted in figures 4 and 5 respectively.

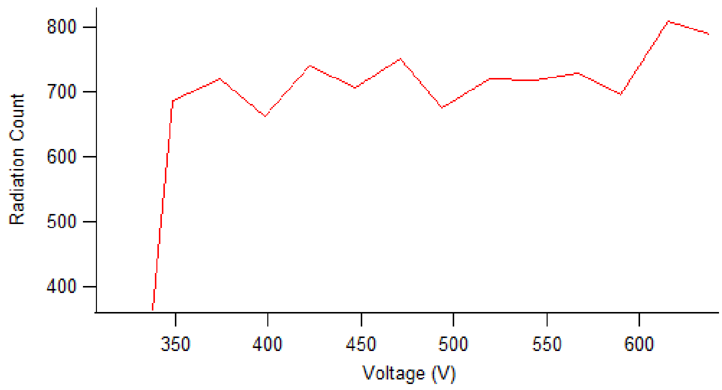

FIG. 4: Radiation count versus the applied voltage for an LND 712 model Geiger tube

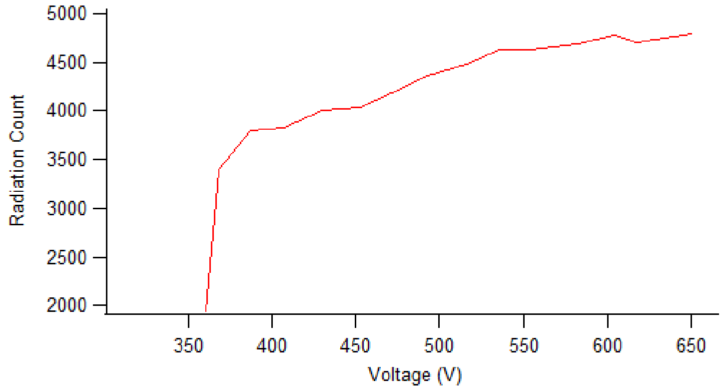

FIG. 5: Radiation count versus the applied voltage for an LND 72314 model Geiger tube

The characteristic data for each Geiger tube is given in table V 16. It was from this data that the decision on the model and operating voltage of the tube was decided for subsequent tests. It can be seen that the slope in the LND 712 model is smaller than that of the LND 72314. Although this is a preferred quality, it was decided that the higher count rate exhibited by the LND 72314 would be more useful than closer to ideal slope, because of this the decision was made to use this model.

Geiger Tube Model	Starting Voltage (V)	Slope (%per V)	% Deviation from Specification
LND 712	349	0.0499	17%
LND 72314	368	0.115	15%

TABLE I: Characteristic data of Geiger Tubes

Sample Calculation for slope

$$Slope = \frac{(\frac{\Delta C}{\Delta V})}{mean\ count\ rate} \times 100\% perV$$

$$\frac{\Delta C}{\Delta V} = \frac{C_2 - C_1}{V_2 - V_1} = \frac{4792 - 3395}{651 - 368} = 4.94$$

$$Slope = \frac{4.94}{4305} \times 100 = 0.115\% perV$$

Measuring the Dead Time

The average values for the count rate of the sources are given below, the uncertainty is taken to be one standard deviation. n_1 represents the difference between the first source count rate and the background count rate, n_2 represents the difference between the second source count rate and the background count rate and n_3 represents the difference between the combined count rate and the background count rate.

$$n_1 = \frac{1472 \pm 108}{60}$$
$$n_2 = \frac{6490 \pm 77}{60}$$
$$n_3 = \frac{7427 \pm 90}{60}$$

$$T = \frac{n_1 + n_2 - n_3}{2n_1 n_2} = \frac{1472 + 6490 - 7427}{2 \times 1472 \times 6490} \cdot 60$$
$$T = 1700 \pm 540 \mu s$$

$$\Delta(n_1 + n_2 - n_3) = \sqrt{108^2 + 77^2 + 90^2} = 160$$
$$\frac{\Delta T}{T} = \sqrt{\left(\frac{160}{535}\right)^2 + \left(\frac{77}{6490}\right)^2 + \left(\frac{108}{1472}\right)^2} = 0.31$$

Statistics of Radioactive Decay

10 Trials

A histogram showing the relative frequency of readings for a sample size of 10 is given in figure 6.

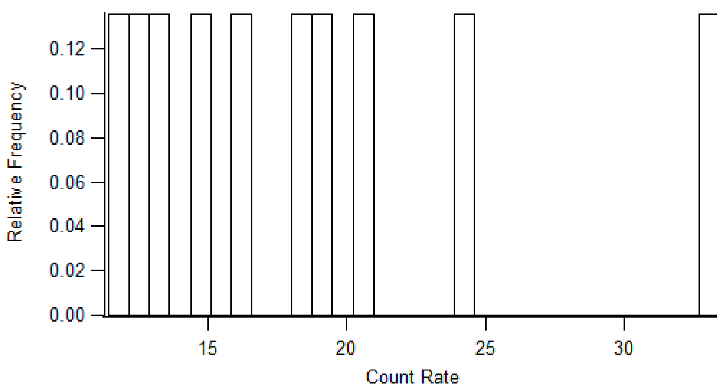

FIG. 6: Relative frequency of count rates for n = 10.

Statistical data for this test is as follows

Mean Count Rate	18
Standard Deviation	6.63
Mean Deviations	4.8

Trial Size	Mean Count	Standard Deviation	Mean Deviations
10	18	6.63	4.8
100	19.5	3.87	3.12
300	19.6	4.39	3.55
500	19.5	4.09	3.32

TABLE II: Statistical data of measured counts over time for different trial sizes

Trial Size	$\sqrt{MeanCount}$	%Difference
10	4.24	36%
100	4.42	14.2%
300	4.43	0.91%
500	4.42	8.06%

TABLE III: Statistical data of measured counts over time for different trial sizes

Trial Size	$\frac{4}{5}\sigma$	%Difference
10	5.3	10%
100	3.096	0.77%
300	3.512	0.01%
500	3.27	1.5%

TABLE IV: Statistical data of measured counts over time for different trial sizes

Trial	% Difference	
Size	$\frac{1}{3}$ deviations $> \sigma$	$\frac{1}{20}$ deviations $> 2\sigma$
10	40%	100%
100	22%	11%
300	15%	33%
500	4.4%	11%

TABLE V: Statistical data of measured counts over time for different trial sizes

1. Standard Deviation $= \sqrt{mean\ count}$

$$\sqrt{mean\ count} = \sqrt{18} = 4.24$$
$$\%_{diff} = \frac{4.24 - 6.63}{6.63} \times 100 = -36\%$$

with a difference of 36%, this statement lacks validity when applied to this particular test.

2. Mean Deviation $= \frac{4}{5}$ *Standard Deviation*

$$\frac{4}{5}\sigma = \frac{4}{5} \times 6.63 = 5.3$$
$$\%_{diff} = \frac{5.3 - 4.8}{4.8} \times 100 = 10\%$$

in this case the standard deviation is found to be 10% greater than the mean deviation. This value indicates conformity with the statement, although the sample size is still too small to draw useful conclusions.

3. $\frac{1}{3}$ *of deviations exceed one standard deviation*

From this data group it is found that 2 out of 10 of the deviations exceed that of the standard deviation. Calculating the % difference between the statement and the findings

$$\%_{diff} = \frac{\frac{1}{5} - \frac{1}{3}}{\frac{1}{3}} \times 100 = -40\%$$

again, with a difference of 40% below the expected values the statement lacks validity when applied to a sample of this size.

4. $\frac{1}{20}$ *of deviations exceed two standard deviations*

It was found that 1 of the 10 deviations exceeded two standard deviations. This value is twice of that expected from the statement.

100 Trials

A histogram showing the relative frequency of count rates for 100 samples is given in figure 7.

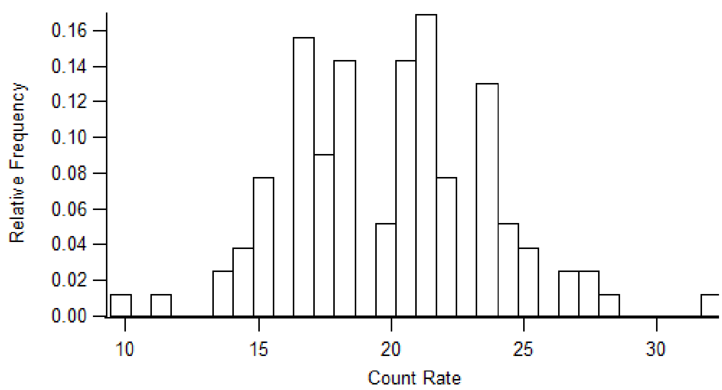

FIG. 7: Relative frequency of count rates for N = 100

Statistical data for this experiment is given below

Mean Count Rate	19.6
Standard Deviation	3.87
Mean Deviation	3.12

5. Standard Deviation $= \sqrt{mean\ count}$

$$\sqrt{mean\ count} = \sqrt{19.6} = 4.42$$
$$\%_{diff} = \frac{4.42 - 3.87}{3.87} \times 100 = 14.2\%$$

a difference of 14%, whilst still not ideal, is far better than previous tests and suggests that a higher sample size may lead to greater agreement between the statements and the results

6. Mean Deviation $= \frac{4}{5}$ *Standard Deviation*

$$\frac{4}{5}\sigma = \frac{4}{5} \times 3.87 = 3.096$$
$$\%_{diff} = \frac{3.096-3.12}{3.12} = -0.77\%$$

a difference of 0.77% below the expected value shows results that strongly agree with the statement. Adding validity to the hypothesis that agreement between statements and results will increase with sample size.

7. $\frac{1}{3}$ *of deviations exceed the standard deviation*

It is found that 26 of the 100 deviations exceed the standard deviation. When compared to the expected value of $\frac{1}{3}$

$$\%_{diff} = \frac{\frac{26}{100} - \frac{1}{3}}{\frac{1}{3}} \times 100 = -22\%$$

although this value has a smaller difference to the expected value than the previous test. The size of the difference still renders it inconclusive.

8. $\frac{1}{20}$ *of deviations exceed two standard deviations*

It is found that 4 of the 100 deviations exceed two standard deviations. When compared to the expected value of $\frac{1}{20}$

$$\%_{diff} = \frac{\frac{4}{100} - \frac{1}{20}}{\frac{1}{20}} \times 100 = -20\%$$

the same is true in this case; although the congruence in this test is better than that of the smaller sample size it is still inconclusive.

200 Trials

A histogram showing the relative frequency of count rates for 200 trials is given in figure 8.

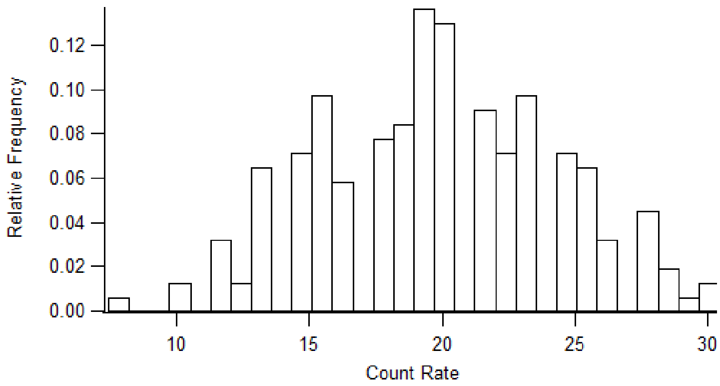

FIG. 8: Relative frequency of count rates for N = 200

Statistical data for this experiment is given below

Mean Count Rate	19.4
Standard Deviation	4.50
Mean Deviation	3.64

9. Standard Deviation $= \sqrt{mean\ count}$

$$\sqrt{mean\ count} = \sqrt{19.4} = 4.40$$
$$\%_{diff} = \frac{4.40-4.50}{4.50} \times 100 = -2.2\%$$

This difference is less than both of the previous tests, in which smaller sample sizes were used. With a difference of 2.2% there is a strong indication of the validity of the statement, as well as the hypothesis that agreement will increase with sample size

10. Mean Deviation $= \frac{4}{5}$ *Standard Deviation*

$$\frac{4}{5}\sigma = \frac{4}{5} \times 4.50 = 3.60$$
$$\%_{diff} = \frac{3.60-3.64}{3.64} = -1.1\%$$

a difference of 1.1% below the expected value shows results that strongly agree with the statement. Although the difference in this value is greater than that for the previous test, the magnitude of the difference is small enough to be accounted for by the random nature of the readings.

11. $\frac{1}{3}$ *of deviations exceed the standard deviation*

It is found that 70 of the 200 deviations exceed the standard deviation. When compared to the expected value of $\frac{1}{3}$

$$\%_{diff} = \frac{\frac{70}{200} - \frac{1}{3}}{\frac{1}{3}} \times 100 = -5\%$$

this value is considerably smaller than those found in tests with smaller sample size. The size of the value suggests agreement with the statement for trials with a greater sample size.

12. $\frac{1}{20}$ *of deviations exceed two standard deviations*

It is found that 6 of the 200 deviations exceed two standard deviations. When compared to the expected value of $\frac{1}{20}$

$$\%_{diff} = \frac{\frac{6}{200} - \frac{1}{20}}{\frac{1}{20}} \times 100 = -40\%$$

the agreement in this test is considerably worse than in previous tests. Due to the general trend towards greater agreement for larger sample sizes, however, I would put this down to the random nature of the readings.

300 Trials

A histogram showing the relative frequency of count rates for 300 samples is given in figure 9.

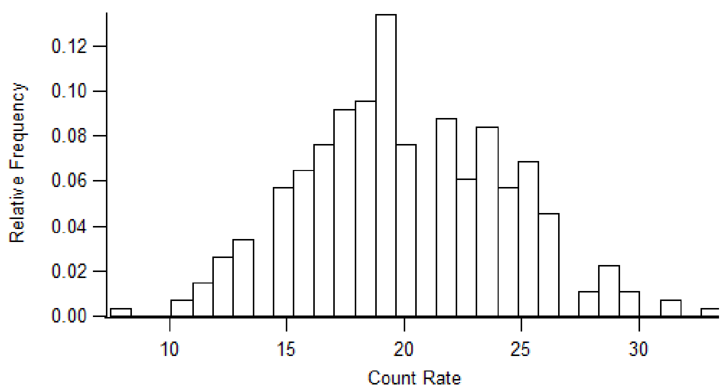

FIG. 9: Relative frequency of count rates for N = 300

Statistical data for this experiment is given below

Mean Count Rate	19.6
Standard Deviation	4.39
Mean Deviation	3.55

13. Standard Deviation $= \sqrt{\textit{mean count}}$

$$\sqrt{mean\ count} = \sqrt{19.6} = 4.42$$
$$\%_{diff} = \frac{4.42-4.39}{4.39} \times 100 = 0.68\%$$

these are very close to each other and are therefore consistent with the statement. This value is also less than all previous tests using smaller sample sizes, consistent with the hypothesis that a greater sample size will increase agreement between results and statements.

14. Mean Deviation $= \frac{4}{5}$ *Standard Deviation*

$$\frac{4}{5}\sigma = \frac{4}{5} \times 4.39 = 3.512$$
$$\%_{diff} = \frac{3.512-3.55}{3.55} = -0.01\%$$

a difference of 0.01% below the expected value shows results that strongly agree with the statement. Adding validity to the hypothesis that agreement between statements and results will increase with sample size.

15. $\frac{1}{3}$ *of deviations exceed the standard deviation*

It is found that 115 of the 300 deviations exceed the standard deviation. When compared to the expected value of $\frac{1}{3}$

$$\%_{diff} = \frac{\frac{115}{300} - \frac{1}{3}}{\frac{1}{3}} \times 100 = 15\%$$

although this value has a smaller difference to the expected value than the previous test. The size of the difference still renders it inconclusive.

16. $\frac{1}{20}$ *of deviations exceed two standard deviations*

It is found that 9 of the 300 deviations exceed two standard deviations. When compared to the expected value of $\frac{1}{20}$

$$\%_{diff} = \frac{\frac{9}{300} - \frac{1}{20}}{\frac{1}{20}} \times 100 = -40\%$$

This value is equal to that of the test with N = 200. Both values have too great of a difference to the expected value to allow us to conclude agreement with the statement. These values are also inconsistent with the hypothesis that a greater sample size will lead to greater agreement.

500 Trials

A histogram showing the relative frequency of count rates for 500 samples is given in figure 10.

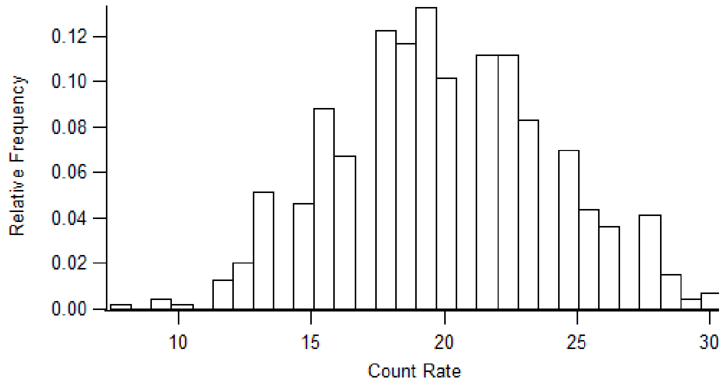

FIG. 10: Relative frequency of count rates for N = 500

Statistical data for this experiment is given below

Mean Count Rate	19.5
Standard Deviation	4.09
Mean Deviation	3.32

17. Standard Deviation $= \sqrt{\textit{mean count}}$

$$\sqrt{\textit{mean count}} = \sqrt{19.5} = 4.42$$
$$\%_{diff} = \frac{4.42-4.09}{4.09} \times 100 = 8.06\%$$

the difference in these values is significantly larger than that of the previous two tests. Although the difference is still small enough to indicate agreement between the statement and the results, it is inconsistent with the hypothesis of agreement increasing with sample size

18. Mean Deviation $= \frac{4}{5}$ *Standard Deviation*

$$\frac{4}{5}\sigma = \frac{4}{5} \times 4.09 = 3.27$$
$$\%_{diff} = \frac{3.27-3.32}{3.32} = -1.5\%$$

a difference of 1.5% below the expected value shows results that strongly agree with the statement. The difference is, however, greater than that for tests of smaller sample sizes.

19. $\frac{1}{3}$ *of deviations exceed the standard deviation*

It is found that 174 of the 500 deviations exceed the standard deviation. When compared to the expected value of $\frac{1}{3}$

$$\%_{diff} = \frac{\frac{174}{500} - \frac{1}{3}}{\frac{1}{3}} \times 100 = 4.4\%$$

the difference between expected and measured values in this test is conclusive with the statement. It is also smaller than previous tests using smaller sample sizes.

20. $\frac{1}{20}$ *of deviations exceed two standard deviations*

It is found that 20 of the 500 deviations exceed two standard deviations. When compared to the expected value of $\frac{1}{20}$

$$\%_{diff} = \frac{\frac{20}{500} - \frac{1}{20}}{\frac{1}{20}} \times 100 = -20\%$$

This value is equal to that of the test with N = 100. Both values have too great of a difference to the expected value to allow us to conclude agreement with the statement. There is also not enough evidence to show that the agreement between this statement and the measured results is increasing with sample size.

Range of Beta Particles in Aluminium

The graph showing the count rate versus thickness of shielding is given in figure 11. From this two linear plots are seen to be intersecting. The rightmost plot is that of the background radiation, whereas the leftmost plot is that of the β radiation. The point at which these plots meet is the range in aluminium for β radiation from a single Chlorine-36 source.

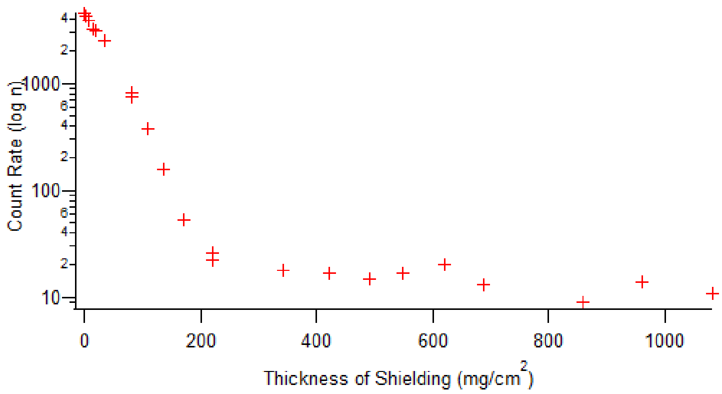

FIG. 11: Count rate versus thickness of aluminium shielding

By observation the range is determined to be $R = 200 \pm 20mg/cm^2$. With the uncertainty an estimated value, allowing for the large inaccuracies associated with measuring a value by eye. When this value is used in comparison on the curve in Halliday, relating energy and range in Al, the energy of β Chlorine-36 radiation is determined to be $E = 0.6 \pm 0.5MeV$. The accepted value for the energy of beta radiation as given in brown is 0.709MeV. Our value is relatively consistent with this with a percentage difference of 15%.

VI. CONCLUSION

Although we found the LND 72314 Geiger tube to be sufficient for our needs and found the increased count number to be beneficial, even though the slope of the LND 72314 at the counting plateau was 0.115% per V compared to the LND 712 at 0.0499% per V which was reflected in the manufacture specifications. The lower slope value found in the plateau would have allowed for more accurate readings with less impact by voltage fluctuations.

Measuring the dead time for the LND 72314 tube was found to be 28 μs, which differs greatly by a factor of 10.

The measured results for the statistics of radioactive decay were consistent with the statements provided by Brown. It was also apparent that for a larger sample size, the agreement between theory and experiment was increased. There were, of course, exceptions to this found in the experiment but nothing that would indicate anything other than the random nature of radioactive emittance.

Graphing the Log of the count rate versus the thickness of the absorber and using this graph we found that the range at which the particles were completely absorbed was about 200 $\pm 20mg/cm^2$. Using Feather analysis, by visually tracing the two parts of the graph, the decreasing count rate and the flat trailing part due to Bremsstrahlung radiation, we were able to find the maximum energy of β radiation from a Chlorine-36 source, was found to be approximately 0.6 $\pm 0.5MeV$, while the accepted value is 0.709MeV, comparatively our value is consistent with only a 15% difference.

VII. REFERENCES

Brown. Counting Systems Handout. 8p.

Glenn F. Knoll. Radiation Detection and Measurement. Fourth Edition. Hoboken, N.J: John Wiley, 2010. 860p.

Jeff Gardiner. Nuclear Counting. Waterloo, Ontario: University of Waterloo; c2013. 3 p.